Comparison of Selected MPPT Techniques Using Different Performance Features

Salauddin Ansari and Om Hari Gupta

Abstract In the last few decades, the tendency and necessity to drift towards renewable sources of energy for power generation have captivated scientists moving to photovoltaic (PV) systems. Since the characteristics of the PV generator is non-linear and its output power changes with solar irradiance and atmospheric temperature, the need for advanced maximum power point tracking (MPPT) technique has always been fascinated. To withdraw the highest power from the PV generators, MPPT is essential. So, to extract the highest power from the photovoltaic generator, even in general situations, maximum power point tracking methods namely perturb and observe, incremental conductance, and temperature control methods are simulated in MATLAB/Simulink. Different parameters of solar energy conversion system—obtained using different algorithms—are compared for different temperatures and irradiances.

Keywords Maximum power point tracking · Perturb and observe · Incremental conductance · Temperature control · Duty ratio

Nomenclature

PV	Photovoltaic
MPPT	Maximum Power Point Tracking
SECS	Solar Energy Conversion System
PO	Perturb and Observe
IC	Incremental Conductance
TC	Temperature Control
MSE	Mean Square Error
FF	Fill Factor
IR	Solar Irradiance

S. Ansari · O. H. Gupta (✉)
Department of Electrical Engineering, National Institute of Technology Jamshedpur, Jamshedpur, Jharkhand, India

S. R. Salkuti and P. Ray (eds.), *Next Generation Smart Grids: Modeling, Control and Optimization*, Lecture Notes in Electrical Engineering 824,
https://doi.org/10.1007/978-981-16-7794-6_4

T	Temperature
d	Duty ratio
MPP	Maximum Power-Point
Δd	Incremental duty ratio
ΔV	Ripple in PV Voltage
ΔP	Ripple in PV Output Power
t_{dpo}	Delay time for PO algorithm
t_{dic}	Delay time for IC algorithm
t_{dtc}	Delay time for TC algorithm
t_{rpo}	Rise time for PO algorithm
t_{ric}	Rise time for IC algorithm
t_{rtc}	Rise time for TC algorithm
t_{ppo}	Peak time for PO algorithm
t_{pic}	Peak time for IC algorithm
t_{ptc}	Peak time for TC algorithm
E_{ppo}	MSE of PV output power for PO algorithm
E_{pic}	MSE of PV output power for IC algorithm
E_{ptc}	MSE of PV output power for TC algorithm
E_{vpo}	MSE of PV voltage for PO algorithm
E_{vic}	MSE of PV voltage for IC algorithm
E_{vtc}	MSE of PV voltage for TC algorithm
E_{ipo}	MSE of PV current for PO algorithm
E_{iic}	MSE of PV current for IC algorithm
E_{itc}	MSE of PV current for TC algorithm
FF_{po}	Fill factor for PO algorithm
FF_{ic}	Fill factor for IC algorithm
FF_{tc}	Fill factor for TC algorithm
η_{ipo}, η_{opo}	Input and Overall efficiency for PO algorithm
η_{iic}, η_{oic}	Input and Overall efficiency for IC algorithm
η_{itc}, η_{otc}	Input and Overall efficiency for TC algorithm

1 Introduction

One of the vast threats of the 21st era is the increasing risk of pollution and drop of energy surety for the upcoming generation. However, since the need for energy continues to increase day by day, we have to take measures and promote new technologies based on yielding energy from sources that are ample and do not endanger the environment. Due to the fullness and sustainability of the sun, solar energy is taking into consideration as one of the sustainable renewable sources at present and future [1–3]. With the advancement in material science, photovoltaic (PV) energy system efficiency continues increasing and the price constantly continues decreasing [4–7].

In addition to many benefits, such as easy installation, no pollution, and easy maintenance, the life of these systems is also very long [8, 9]. The technical improvements in the photovoltaic system have decreased the price and increased the solar energy conversion system (SECS) efficiency. There is still a long way to reach the desired level of energy generation. Some of the important studies to harvest a maximum of available power out of the PV system i.e., MPPT algorithms are included in this chapter.

The MPPT plays a very important role in solar power generation since it extracts maximum power output from its PV system for different atmospheric situations and thereby, maximizing the system's efficiency. In this way, MPPT can reduce the total cost of the entire system. The MPPT technique continuously searching the operating point corresponding to maximum power output and keep it at that point. Several MPPT techniques are introduced in the literature [10–12]. However, the perturb and observe (PO) and incremental conductance (IC) are the two specific methods and remain the most extensively used methods in commercial photovoltaic MPPT systems. Apart from these two, a temperature control (TC)-based MPPT method is also discussed in this chapter. The main emphasis of this study is the comparison of the aforementioned MPPT techniques for SECS by considering various features/parameters. These features/parameters are as follows:

- PV voltage and its ripple
- PV current and its ripple
- PV power and its ripple
- delay time, rise time, and peak time
- PV internal and overall efficiency
- mean square error (MSE)
- fill factor (FF).

The remaining chapter is formulated according to the following. Section 2 introduced the different parameters/terms related to SECS. Section 3 presents the working principle of SECS. Section 4 describes different MPPT techniques, Sect. 5 describes heuristic approaches of the MPPT Technique and then, in Sect. 6, results and discussions are included. Finally, the Conclusion is added to Sect. 7.

2 Different Parameters Related to SECS

- **Fill factor**: The fill factor (FF) is a figure of merit of PV cell. It tells how good or how bad a PV cell is. Figure 1 depicts the concept of fill factor. The FF is nothing but a ratio of maximum accessible power ($V_{\mathrm{mpp}} \times I_{\mathrm{mpp}}$) to the maximum theoretical power ($V_{\mathrm{oc}} \times I_{\mathrm{sc}}$). Mathematically, it can be written as given in (1).

$$FF = \frac{\left(\mathrm{V}_{mpp} \cdot \mathrm{I}_{mpp}\right)}{\left(\mathrm{V}_{oc} \cdot \mathrm{I}_{oc}\right)} \tag{1}$$

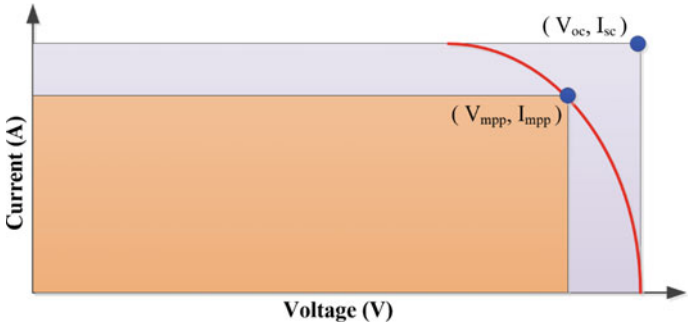

Fig. 1 Fill factor representation

- **MSE**: It is the mean of the squares of the errors—that is, the mean squared changes between the predicted value and the true value. Mathematically, MSE can be written as

$$\mathrm{MSE} = \frac{1}{\mathrm{n}} \sum_{\mathrm{i}=1}^{\mathrm{n}} \left(\mathrm{X_i} - \hat{\mathrm{X}} \right) \tag{2}$$

where n is the no. of samples of data points
X is the vector of true value
$\hat{\mathrm{X}}$ is the vector of the predicted value.

- **Delay time**: The delay time is termed as the amount of time needed for the response of a system to reach 50% of its final value within the first cycle of oscillation.
- **Rise time**: The rise time is termed as the amount of time needed for the response of a system to reach from 10% of its final value to 90% of its final value within the first cycle of oscillation.
- **Peak time**: The peak time is termed as the amount of time needed for the response of a system to reach its first peak.

Different times i.e., delay time (t_d), rise (t_r) and peak time (t_p) are depicted in Fig. 2.

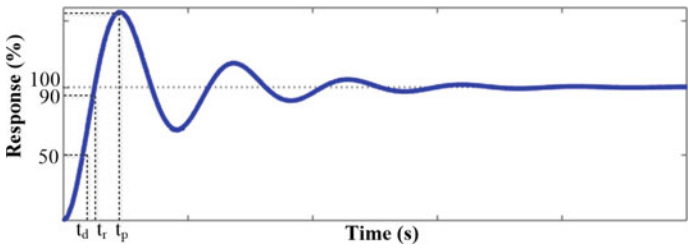

Fig. 2 Delay time (t_d), rise time (t_r), and peak time (t_p)

3 Working Principle of Solar Energy Conversion System

The Photovoltaic panels are made up of semiconductor material designed to transform solar irradiation into usable electrical energy. Since the solar irradiance (IR) and temperature (T) randomly changes throughout the day, the power output also changes. Figure 3 explains the concept of a solar energy conversion system that represents the block diagram of SECS which comprises of PV panel, MPPT controller, DC–DC boost converter connected through DC load R_L. When sun light falls on the PV panel, it generates PV voltage V_{pv} and current I_{pv} which has nonlinear relation as illustrated in Fig. 4. To withdraw the maximum available electrical power from the PV panel, an MPPT controller is employed. MPPT controller senses the PV voltage "V_{sense}" and current "I_{sense}" and next computes the optimum duty ratio (d) corresponding to the MPP which modifies the input impedance of boost converter.

Finally, the boost converter is cascaded with DC load, R_L to transfer power to the load R_L. The variations in PV current, power, and impedance with PV voltage are illustrated in Fig. 4, where slopes S_1 and S_2 represent the load lines—one corresponding to the fixed load impedance (S_1) and another corresponding to load impedance modulated by the boost converter (S_2). The slope S_1 will be equal to $1/R_L$ while slope S_2 will be $1/R_L(1-d)^2$. If load "R_L" is directly coupled to the PV panel it may extract the power P_1 which is not the maximum available power. To the withdraw maximum power from the PV panel, the DC–DC boost converter is introduced between the PV panel and the load R_L which modulates the load impedance to $R_L(1-d)^2$. Alternatively stated, the converter is shifting the operating point along the locus of maximum power point (MPP) and fixing the operating point at MPP. Hence, the maximum power "P_{mpp}" is extracted from the PV panel. From Fig. 4, it is clear that if we have to shift the operating point at MPP, the slope of the line should be decreased and the input impedance of converter $R_{in} = R_L(1-d)^2$ should be increased. To increase R_{in}, d must be decreased, until the MPP is reached. After the measurement of voltage and current, the MPPT technique computes d so as to transfer maximum power to the load. The converter chosen can also be a boost, buck, or buck-boost converter, but in this chapter, a boost converter is employed, due to its greater efficiency and higher range control [13].

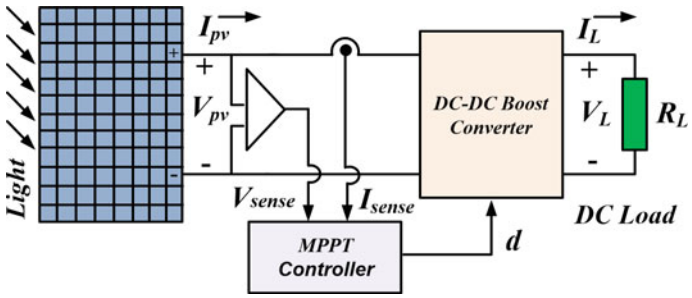

Fig. 3 Equivalent diagram of a SECS with MPPT

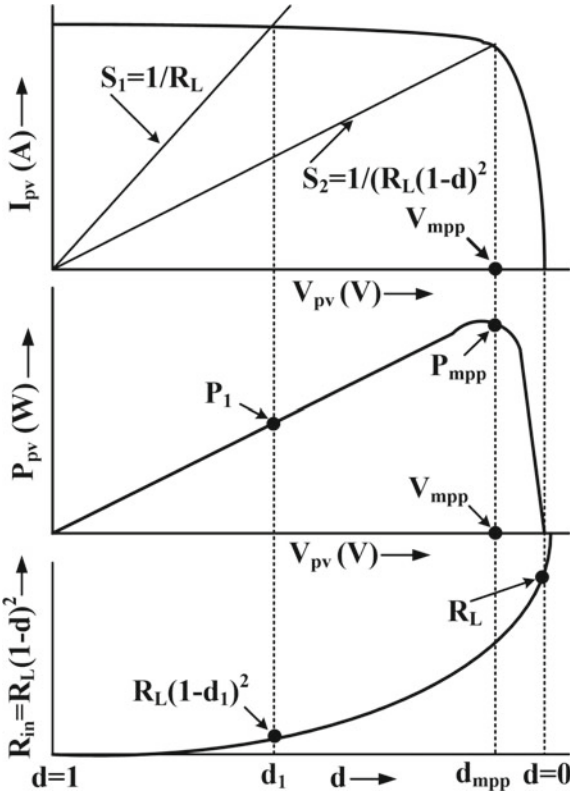

Fig. 4 Intersection between load line, current–voltage, and power–voltage curve

4 MPPT Techniques

Three MPPT techniques are included for comparative analysis and discussed next.

4.1 Perturb and Observe

The perturb and observe (PO) [14–19] technique is the most frequently used and discussed MPPT technique. In this method, initially, the PV output voltage $V(\mathrm{k})$ and current $I(\mathrm{k})$ are captured, and then PV output power $P(\mathrm{k}) = V(\mathrm{k}) \times I(\mathrm{k})$ is calculated. From calculated power and voltage, the change in PV output power "ΔP" and voltage "ΔV" are obtained as follows:

$$\Delta \mathrm{P} = \mathrm{P}(K) - \mathrm{P}(K-1) \tag{3}$$

$$\Delta \mathrm{V} = \mathrm{V}(K) - \mathrm{V}(K-1) \tag{4}$$

Now, if the changes in PV output power and voltage are zero i.e., $\Delta P = 0$ and $\Delta V = 0$, the algorithm returns to the start position. If the change in PV output power is negative i.e., $\Delta P < 0$, the change in voltage will be checked. Now, if $\Delta V < 0$, the operating voltage is increased else it will be decreased. While if the change in PV output power is not negative i.e., $\Delta P \geq 0$, the change in the voltage (ΔV) is checked, and if $\Delta V < 0$, the operating voltage is decreased else it will be increased. After shifting the operating voltage, the algorithm returns to the start position. The corresponding flow diagram is given in Fig. 5. The PO technique has two primary drawbacks. Initially, the value of perturbation given to the system is crucial and determines the amount of oscillations under steady-state at MPP. Besides, the speed of convergence of output power towards MPP is slower. The greater the perturbations, quickly the algorithm finds the MPP. However, greater perturbation results in a high value of oscillation at MPP.

At the same time, if the value of perturbation is too small, the oscillation about MPP will decrease, though the speed of convergence towards MPP will also decrease. This means that there will be a compromise among the speed of convergence and steady-state oscillations.

To resolve this drawback, the amount of perturbation may be decreased as it approaches towards the MPP—the same is proposed in [20, 21]. When the output power is far-off from the MPP, larger perturbations are used while smaller perturbations are used when the output power is closed to MPP. Overall, the amount of perturbations is selected based on the power–current curve slope. However, it results in complexity and a costly technique. Further, whenever the operating point of the system changes rapidly, the method can settle to an erroneous operating point. To resolve such drawbacks, different methods have been proposed [22, 23]. The key facts related to PO algorithm are:

(a) Two sensors are required, one, for voltage and the other for current.
(b) Slow rate of convergence to MPP.
(c) It fails to follow MPP if the environmental conditions vary quickly.
(d) Under steady-state, response will be oscillatory about the MPP.

4.2 Incremental Conductance

The IC [24–28] technique uses the slope of the power–voltage curve of the PV generator to track MPP. The slope of the power–voltage curve (Fig. 4) of the PV panel is zero at MPP. The slope will be positive if the PV output power is less than MPP and negative if the PV output power is more than MPP. Mathematically, can write the aforementioned discussion as given below in Eq. (5).

$$\left.\begin{array}{l} \frac{d\mathrm{P}}{d\mathrm{V}} = 0;\ at\ MPP \\ \frac{d\mathrm{P}}{d\mathrm{V}} > 0;\ left\ of\ MPP \\ \frac{d\mathrm{P}}{d\mathrm{V}} < 0;\ right\ of\ MPP \end{array}\right\} \tag{5}$$

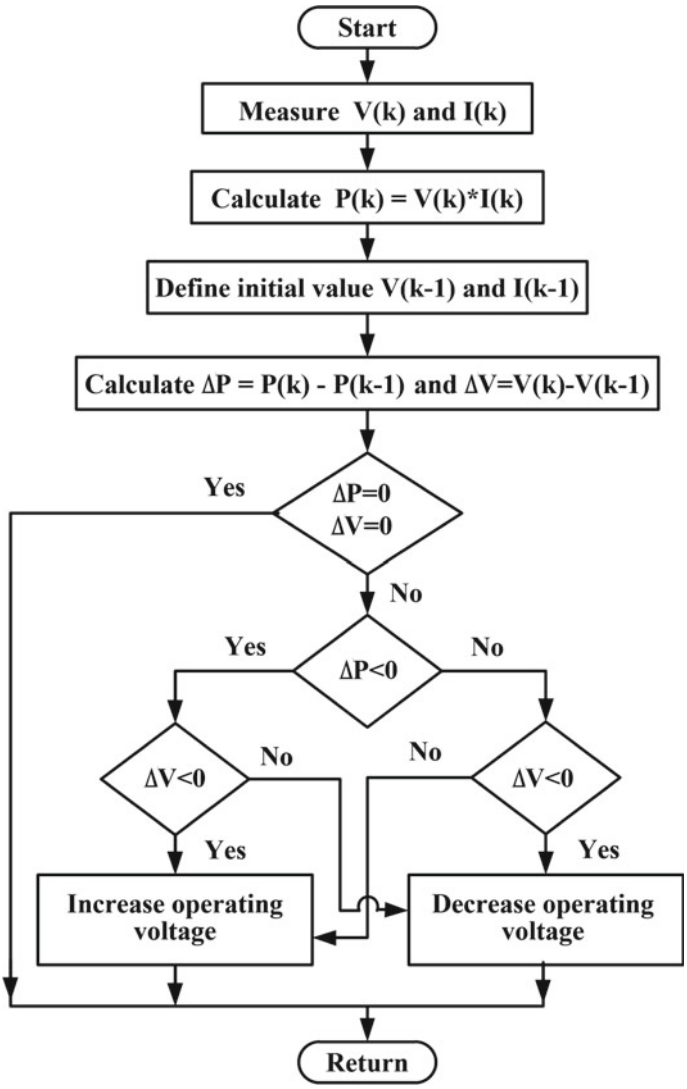

Fig. 5 Flow diagram of PO algorithm

For maximum output power, the PV output power differentiation with respect to voltage should be zero, i.e.:

$$\frac{dP}{dV} = \frac{d(VI)}{dV} = I + V\frac{dI}{dV} \cong I + V\frac{\Delta I}{\Delta V} = 0 \tag{6}$$

Equation (6) can be modified as given in (7) below.

$$\frac{\Delta \mathrm{I}}{\Delta \mathrm{V}} \cong \frac{-\mathrm{I}}{\mathrm{V}} \tag{7}$$

Now, Eq. (5) can be expressed as:

$$\left.\begin{array}{l} \frac{\Delta \mathrm{I}}{\Delta \mathrm{V}} = \frac{-\mathrm{I}}{\mathrm{V}};\ at\ MPP \\ \frac{\Delta \mathrm{I}}{\Delta \mathrm{V}} > \frac{-\mathrm{I}}{\mathrm{V}};\ left\ of\ MPP \\ \frac{\Delta \mathrm{I}}{\Delta \mathrm{V}} < \frac{-\mathrm{I}}{\mathrm{V}};\ right\ of\ MPP \end{array}\right\} \tag{8}$$

Thus, it is possible to detect whether the PV generator is working at MPP, left of MPP, or right of MPP. So, as per Eq. (8), the MPP can be tracked by comparing instantaneous conductance (I/V) with the incremental conductance ($\Delta I/\Delta V$). The flow diagram of the IC method is given in Fig. 6. Initially, PV output voltage V(k) and current I(k) are captured. Then the initial and old values of voltage and current are updated. From the captured voltage and current, ΔV is determined as given in (4) and ΔI is determined as given in Eq. (9) below.

$$\triangle\ \mathrm{I} = \mathrm{I}(K) - \mathrm{I}(K-1) \tag{9}$$

Now, if the change in PV output voltage is zero i.e., $\Delta V = 0$, the change in the current ΔI is to be checked, and if $\Delta I = 0$, the algorithm returns to the start position. If $\Delta I > 0$, the operating voltage is to be decreased else it is to be increased. While if PV output voltage is not zero i.e., $\Delta V \neq 0$, the change in ($\Delta I/\Delta V$) and instantaneous conductance (I(k)/V(k)) are checked and if $\Delta I/\Delta V = -I$(k)/V(k), the algorithm returns to the start position. If $\Delta I/\Delta V > -I$(k)/V(k), the operating voltage is increased else it will be decreased. The speed of tracking the MPP depends upon the amount of change in the magnitude of operating voltage. If increment or decrement in operating voltage is large, the algorithm tracks the MPP faster but the system cannot remain at MPP but oscillates around it. If the size of increment or decrement in operating voltage is too small, the response becomes slower but the oscillations close to MPP are lesser. So, again, there is a compromise between the speed of convergence and oscillations. There are mainly two advantages of this algorithm, first, it gives effective results even during the rapid change in atmospheric conditions. Second, it has low oscillations about MPP as compared to the PO algorithm. The main drawback of this technique is that it requires complex control circuitry. The key facts related to this algorithm are:

(a) Two sensors are required—one for voltage another for current.
(b) More complicated than the PO algorithm.
(c) Fast dynamic tracking regardless the atmospheric conditions.
(d) Under steady-state, lesser oscillations about the MPP.

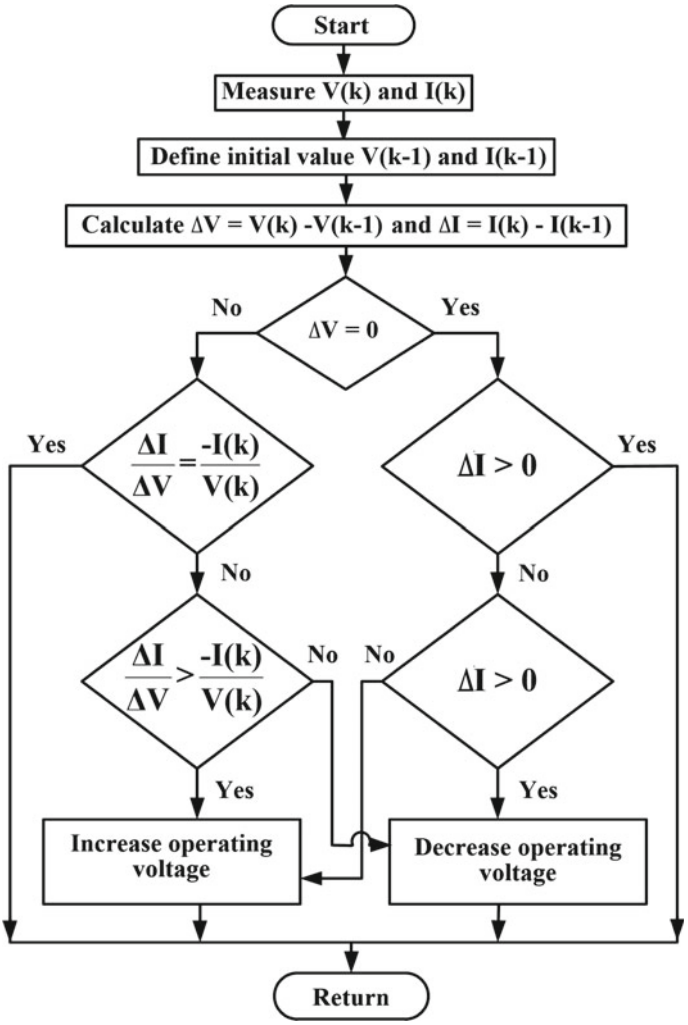

Fig. 6 Flow diagram of the IC algorithm

4.3 Temperature Control

The TC [29–31] technique is originated on the concept that the output voltage of the PV module depends on the surface temperature of the PV panel. The relation is described by Eq. (10) below [32].

$$\mathrm{V}_{mpp}(T) = \mathrm{V}_{mpp}(T_o) + \alpha_{Vmpp}(T - T_o) \tag{10}$$

$$\Delta \mathrm{d} = \left[\mathrm{V} - \mathrm{V}_{mpp}(T)\right] \mathrm{S}_{\Delta d} \tag{11}$$

$$\mathrm{d}(k) = \Delta\mathrm{d} + \mathrm{d}(k-1) \tag{12}$$

where

$V_{\mathrm{mp}p}(T)$	MPP voltage at the measured temperature
$V_{\mathrm{mpp}}(T_o)$	MPP voltage at a measured temperature from the datasheet
α_{Vmpp}	Temperature coefficient from the datasheet
T	Measured temperature
$\mathrm{T_o}$	Reference temperature from the datasheet.

From Eq. (10), it is obvious that MPP voltage V_{mpp} relies on the measured temperature T because $V_{\mathrm{mpp}}(\mathrm{T_o})$, α_{Vmpp}, and $\mathrm{T_o}$ are the datasheet information. The flowchart used to implement the TC technique is described in Fig. 7. First, the system starts to sense the PV output voltage V and PV module surface temperature T. With the help of measured temperature T, the optimized value of MPP voltage $V_{\mathrm{mpp}}(\mathrm{T})$ is calculated from Eq. (10). Also, the incremental duty ratio (Δd) is proportional to the change in the actual PV module output voltage V and the desired MPP voltage $V_{\mathrm{mpp}}(\mathrm{T})$ according to Eq. (11). Where constant $S_{\Delta\mathrm{d}}$ is the step size of Δd and the value of $S_{\Delta\mathrm{d}}$ decides the convergence rate of the technique. For a higher value of $S_{\Delta\mathrm{d}}$, the algorithm tracks the MPP faster and for a smaller value of $S_{\Delta\mathrm{d}}$, it tracks the MPP at a slower rate. Finally, to ensure the PV output voltage to be as near as possible to MPP voltage V_{mpp}, $d(\mathrm{k})$ is upgraded according to Eq. (12) which is the sum of the Δd and the previous value of duty ratio $d(\mathrm{k}-1)$. Now, $d(\mathrm{k})$ and minimum duty ratio (d_{min}) are compared and if the duty ratio is less than the minimum duty ratio i.e., $d(\mathrm{k}) < d_{\mathrm{min}}$, it is updated as $d(\mathrm{k}) = d_{\mathrm{min}}$ and then the algorithm returns to the start position. While if the duty ratio is greater than the maximum limit i.e., $d(\mathrm{k}) > d_{\mathrm{max}}$, it is again limited to d_{max} and then the algorithm returns to the start position. Else if the duty ratio is within the upper and lower limits, the algorithm returns to the start position.

Since the temperature on the PV panel changes gradually because of the thermal inertia, the voltage of the PV terminal will also change smoothly. At the same time, the PV output current is directly in proportion to the surface IR; therefore, its dynamic is faster than the dynamics of temperature. Thus, it is obvious that the PV output power includes two separate dynamics due to the slow change in temperature and the fast fluctuations of the IR. However, when the TC technique is used, only temperature measurements are taken into account. Therefore, fast dynamics is eliminated from the technique and makes tracking more smooth, stable, and faster.

The key facts related to this algorithm are:

(a) Two sensors are required one for voltage other for temperature.
(b) It is constructed on the concept that the PV output voltage is directly related to the temperature.
(c) Here, only the slow dynamic is taken into consideration and the fast dynamic is eliminated and therefore, the tracking trend is more smooth, stable, and faster.

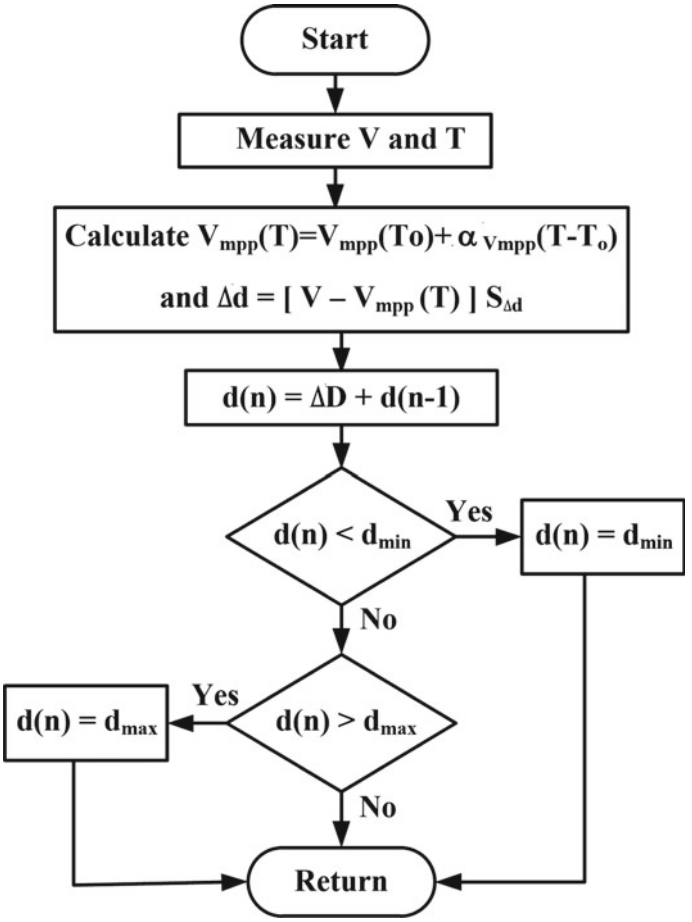

Fig. 7 Flow chart of TC algorithm

5 Implementation of Heuristic Approaches of the MPPT Technique

Figure 8 shows the implementation of heuristic approaches of the MPPT Technique which is composed of a PV panel, MPPT controller, Boost converter, load, and filter connected to the utility grid. Initially, solar energy is converted to electrical energy with the help of a solar panel. Then, output voltage and current of the solar panel are measured—which are utilized by the MPPT controller to produce a duty cycle for the Boost converter corresponding to its maximum power. Since the output of the Boost converter is DC in nature so to convert it into AC, an inverter is used. An inverter control block generates switching pulses for the inverter by utilizing the output voltage and current of the inverter. Therefore, the SECS generate AC active

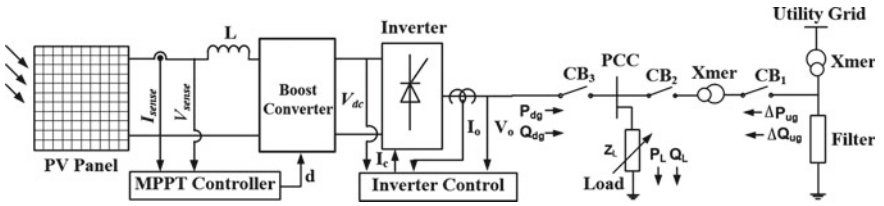

Fig. 8 Implementation of heuristics approaches of the technique

power (P_{dg}) and reactive power (Q_{dg}). A local load is connected to the system then finally, SECS is attached to the utility grid through a step-up transformer. A filter is used to eliminate any lower order harmonics from the supply. If the load is less than the generated power of SECS then surplus power ΔP_{ug} and ΔP_{ug} are supplied by the utility grid.

6 Results and Discussion

For the verification of all three algorithms i.e., PO, IC, and TC, MATLAB/Simulink simulations were executed considering a readily available PV module 'Sun Earth Solar Power TPB156*156-60-P225W'. The DC–DC boost converter is employed for MPPT. The electrical specifications of the PV panel are presented in Table 1 and the PV Power, voltage, and current, obtained from the power–voltage curve, are given in Table 2. To obtain a comparative analysis, two aspects are taken into consideration i.e., changes in IR and temperature. The influence of change in IR and temperature on different parameters such as voltage, current, power, ripples in voltage, current, and power are recorded in the present analysis. Moreover, Mean Squared Error (MSE), Fill factor (FF), delay time, rise time, peak time, internal (or PV) efficiency, and overall efficiency are also obtained. Different results of the mentioned cases are included next.

6.1 Voltage and Voltage Ripples in Varying Atmospheric Conditions

Figure 9 represents the PV output voltages obtained for PO, IC, and TC algorithms (i.e., V_{po}, V_{ic}, and V_{tc} respectively) at a fixed temperature (25 °C) and varying IR. It can be observed from Fig. 9 that as the IR rises from 400 to 1200 W/m^2 in the steps of 200, PV output voltages by PO and IC algorithms (i.e., V_{po} and V_{ic}, respectively) are decreased slightly while that of TC algorithm (V_{tc}) has increased. It is also found that the TC algorithm gives slightly lesser PV output voltages for IR of 400–600 W/m^2 while for 800–1200 W/m^2, all the three algorithms gave approximately the same

Table 1 Specifications of 'Sun Earth Solar Power TPB156*156-60-P225W' PV module

Array data	
Parallel string	2
Series connected module per string	2
Module data	
Maximum power P_{max}	225.04 W
Voltage at MPP V_{mpp}	29 V
Current at MPP I_{mpp}	7.76 A
Voltage in open circuit condition V_{oc}	36.5 V
Temperature coefficient of V_{oc}	−0.34/°C
Short circuit current I_{sc}	8.26 A
Temperature coefficient of I_{sc}	0.07/°C
Cells per module	60
Module parameters	
Current due to light I_{lt}	8.2671 A
Saturation current through diode I_o	$1.3914 * 10^{-10}$ A
Diode ideality factor	0.95481
Resistance in shunt R_{sh}	476.1198 Ω
Resistance in series R_{se}	0.41169 Ω

Table 2 PV power, voltage and current at different temperature T and irradiance IR obtained from PV curve

T (°C)	IR (W/m^2)	P_{pv} (W)	V_{pv} (V)	PV current (A)
25	400	367.3	58.9	6.236
25	600	550	58.78	9.357
25	800	727.9	58.54	12.43
25	1000	900.2	58	15.52
25	1200	1066	57.4	18.58
30	1000	881.6	56.67	15.56
40	1000	864.1	54.18	15.58
50	1000	806.3	51.69	15.6

PV output voltages. Figure 10 shows the PV output voltages for the variations in temperature (30, 40, and 50 °C) with IR kept constant at 1000 W/m^2. It is found that as the temperature increases, PV output voltages obtained from PO, IC and TC algorithms decrease. It is also observed that the TC algorithm gives slightly less PV output voltage as well as slightly fewer ripples in PV output voltage as compared to PO and IC algorithms.

For better comparative analysis, Fig. 11 includes the comparison bars of PV voltages obtained from different MPPT techniques and the PV voltage, corresponding

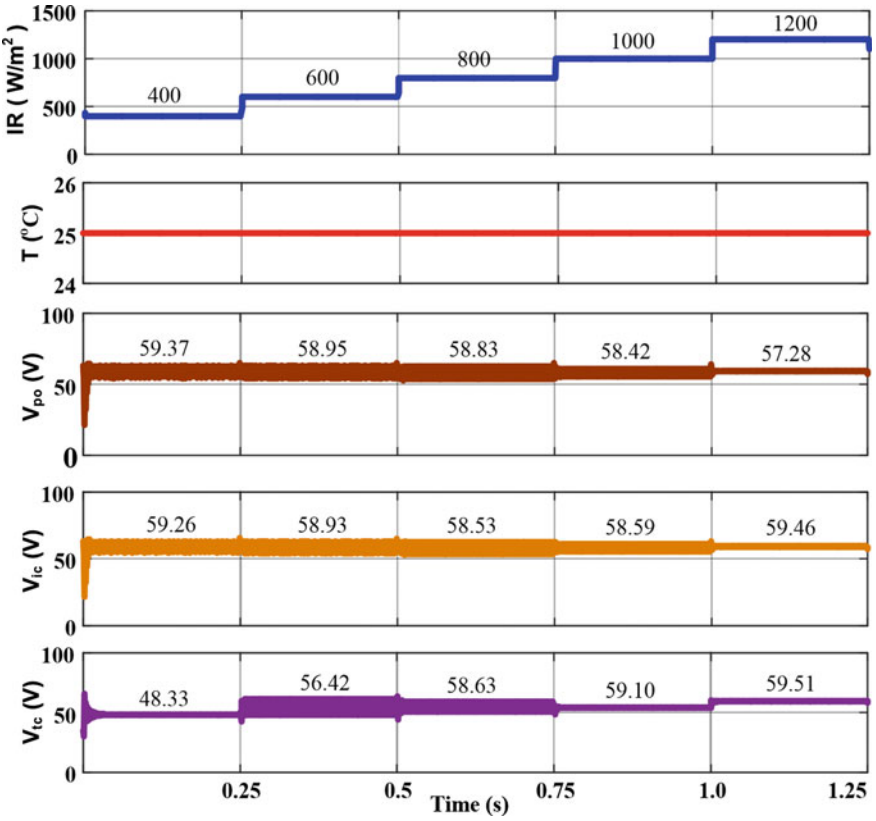

Fig. 9 PV output voltage with PO, IC, and TC algorithm when irradiance varied

to MPP i.e., V_{pv}—obtained from the PV characteristicsfor a given temperature and IR. It can be concluded that all the methods give quite accurate results. In some of the cases, particularly at 25 °C and 1200 W/m^2, the voltages obtained from PO, IC, and TC methods are equal and slightly more than V_{pv}. Similarly, Fig. 12 represents the ripple in PV voltage ΔV at different temperatures and IR for different methods. It is observed that minimum ripples are there in the case of the TC method, followed by IC and PO methods. It is also observed that as the temperature and IR are increased, the value of ripples in PV voltage decreases. For example, at 25 °C and 400 W/m^2, the ripples in PV voltage (ΔV) is about 7 V but at 40 °C and 1000 W/m^2, its value is about 2 V.

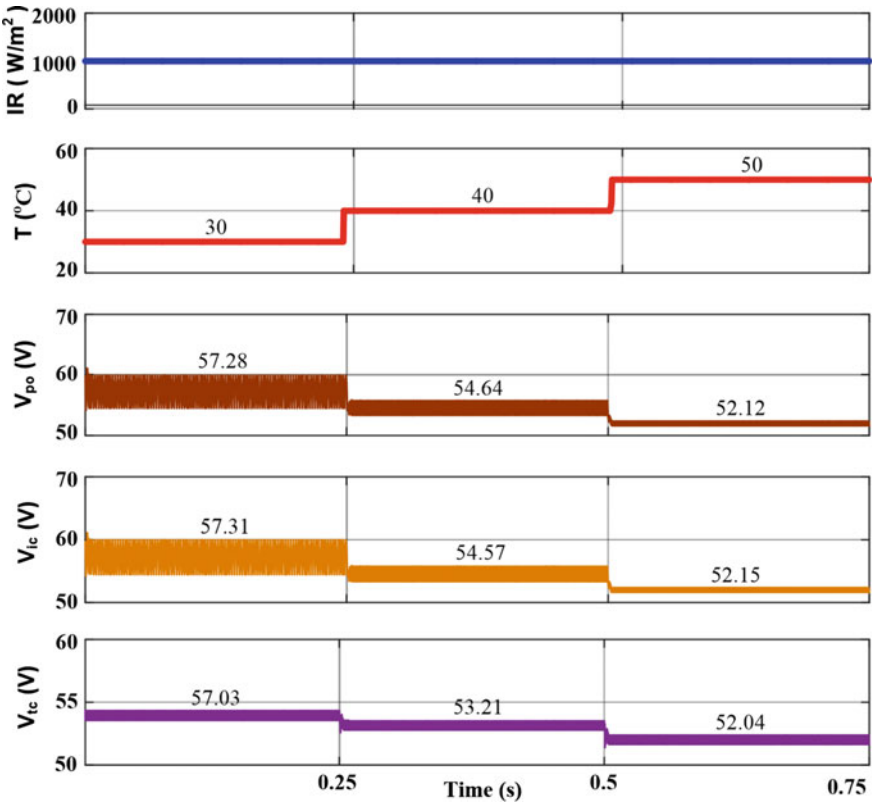

Fig. 10 PV output voltage with PO, IC, and TC algorithm when temperature varied

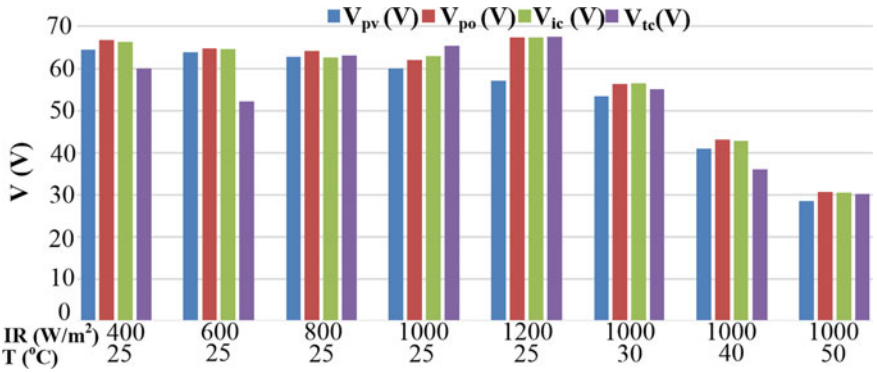

Fig. 11 Comparison of PV output voltage with PO, IC, and TC algorithm when both temperature and irradiance are varied

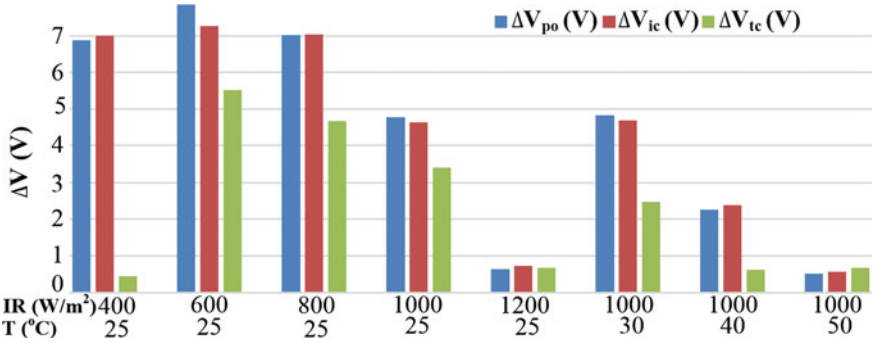

Fig. 12 Ripple in PV output voltage with PO, IC, and TC algorithm when both temperature and irradiance are varied

6.2 *Power and Power Ripples in Varying Atmospheric Conditions*

Figure 13 represents the PV output powers P_{po}, P_{ic} and P_{tc} obtained for PO, IC, and TC algorithms, respectively at 25 °C and different IR (400–1200 W/m^2). It can be noticed from this figure that all three techniques successfully track the MPP and as the IR increases, PV output power also increases. For example, for time 0.75 s to 1 s, the PV output power obtained from PV characteristics (P_{pv}) is 900.2 W—given in Table 2—while PO, IC, and TC algorithms (i.e., P_{po}, P_{ic}, P_{tc}, respectively) provide 891.25 W, 890.95 W and 892 W of power, respectively. The obtained powers are very close to P_{pv}. Initially, due to the presence of transients from 0 to 0.25 s, the TC algorithm provides lesser PV output power as compared to that of IC and PO algorithms. Figure 14 presents PV output powers for different temperatures (30, 40, and 50 °C) with a fixed IR of 1000 W/m^2. It can be noted from the figure that, even in transient-period i.e., from 0 to 0.25 s, power by TC algorithm is almost equal to P_{pv}—providing the most accurate result in comparison to other methods. Moreover, for better understanding, PV output powers obtained from different algorithms at different temperatures and IR are compared magnitude wise in Fig. 15. Finally, Fig. 16 represents the ripples in PV output powers for different algorithms under the same environmental conditions. It can be noticed that ripples in output power ΔP are maximum at 25 °C and 800 W/m^2 which is about 27 W while it is minimum at 50 °C and 1000 W/m^2 which is about 2 W. That means upon increasing the IR and temperature, ripples in PV output power (ΔP) decreases.

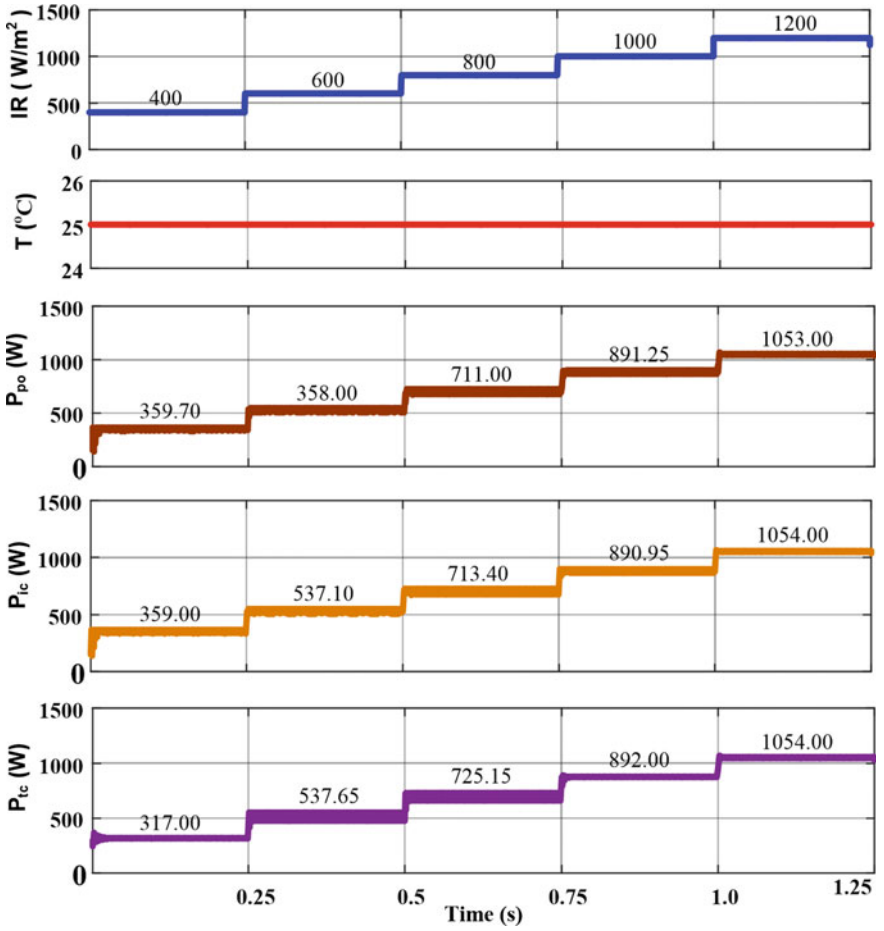

Fig. 13 PV output power with PO, IC and TC algorithm when irradiance is varied

6.3 Current and Current Ripples in Varying Atmospheric Conditions

Figure 17 shows the comparison of PV currents obtained from PO, IC, and TC methods (I_{po}, I_{ic}, I_{tc}, respectively) with ideal PV current obtained from characteristic I_{pv} for different temperatures and IR. It is found that all the three algorithms work similarly and the currents are almost the same as obtained from PV characteristic (I_{pv}). It is also noticed that as the IR increases, the PV output current goes on increasing while it is almost constant if IR is kept constant and only the temperature is varied. Further, Fig. 18 represents the ripples in the PV output currents for changed IR and temperature. It can be noticed in this figure that ripples in PV output current

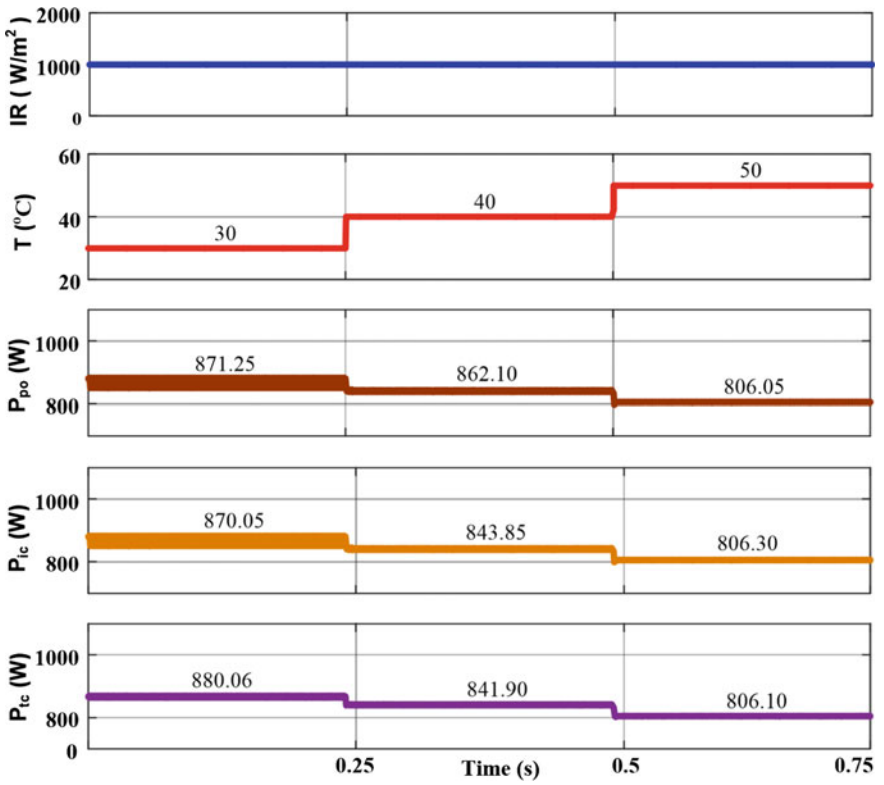

Fig. 14 PV output power with PO, IC and TC algorithm when the temperature is varied

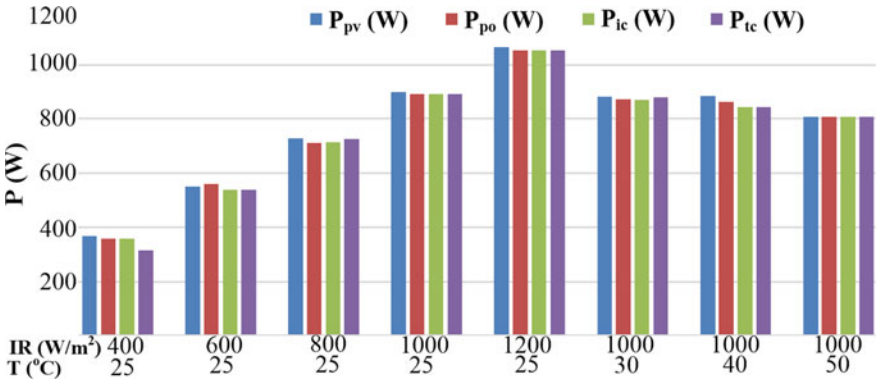

Fig. 15 Comparison of PV output power with PO, IC and TC algorithm when both temperature and irradiance are varied

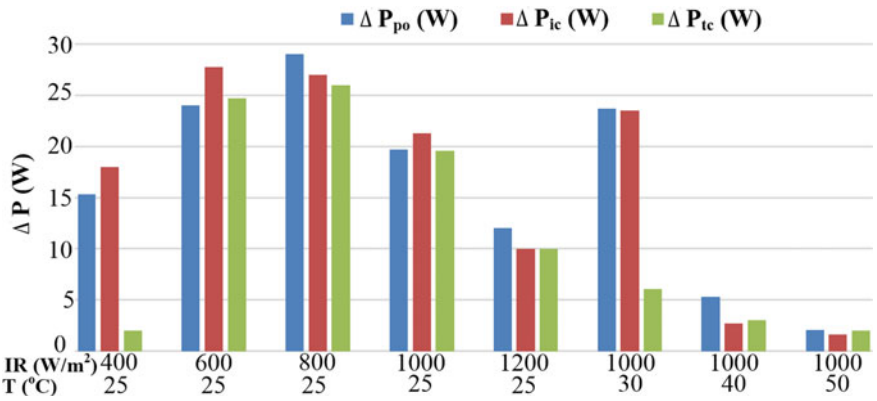

Fig. 16 Ripple in PV output power with PO, IC and TC algorithm when both temperature and irradiance are varied

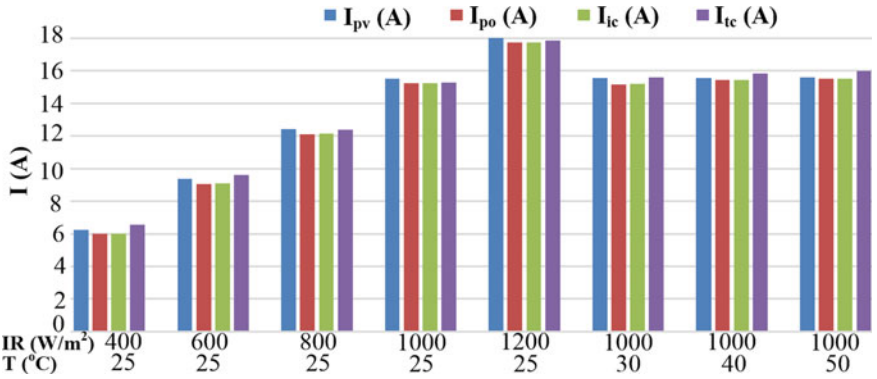

Fig. 17 Comparison of PV output current with PO, IC, and TC algorithm when both temperature and irradiance are varied

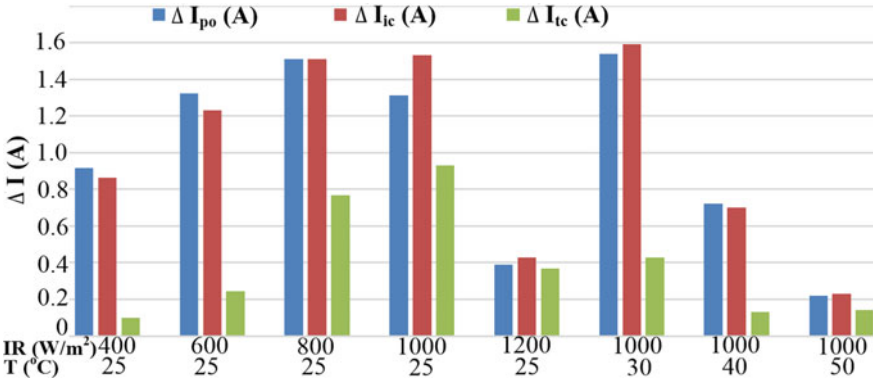

Fig. 18 Ripple in PV output current with PO, IC, and TC algorithm when both temperature and irradiance are varied

by the TC algorithm are minimum as compared to that of PO and IC algorithms. The ripples in PV output currents obtained from PO and IC algorithms are almost equal.

6.4 Tracking Performance and Efficiency

Figure 19 presents the delay times, rise times, and peak times for PO, IC, and TC algorithms which give an idea about the tracking performances of the MPPT methods. It can be observed from this figure that the delay time is minimum for the TC algorithm (i.e., t_{dtc})—equal to 0.415 ms. The rise time is minimum for the IC algorithm (i.e., t_{ric})—equal to 2.465 ms whereas the peak time is minimum for PO method (i.e., t_{ppo})—equal to 2.94 ms. Figure 20 shows the mean squared errors (MSEs) for PV output power, voltage, and current for PO, IC, and TC algorithms (considering 1000 samples for each case). The MSE of PV output powers for all methods (i.e., E_{ppo},

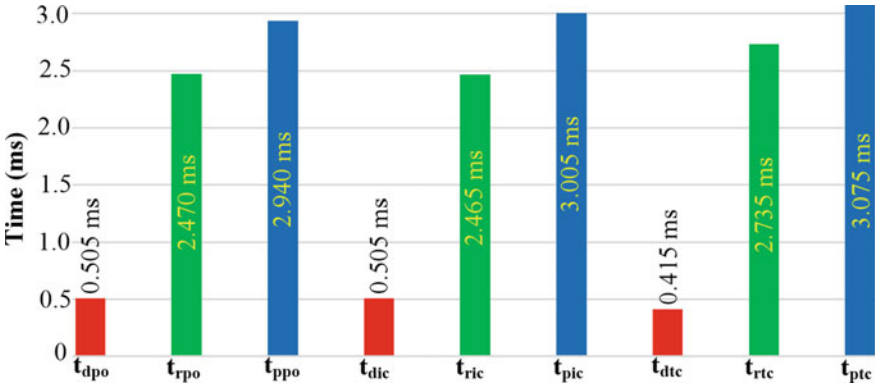

Fig. 19 Delay time, rise time, and peak time with PO, IC, and TC algorithm

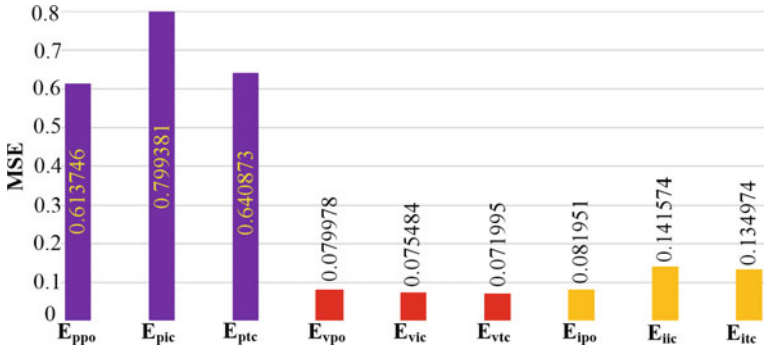

Fig. 20 MSE of PV output power, voltage, and current with PO, IC, and TC algorithm

E_{pic}, and E_{ptc} for PO, IC, and TC algorithms, respectively) are calculated and it is found that, out of them, MSE is minimum for the PO algorithm.

Similarly, MSEs for the PV output voltages (i.e., E_{vpo}, E_{vic}, and E_{vtc} for PO, IC, and TC algorithms, respectively) are calculated and it is found that all the methods have almost the same voltage MSE. Finally, MSEs for the PV output currents (i.e., E_{ipo}, E_{iic}, and E_{itc} for PO, IC, and TC algorithms, respectively) are calculated and it is observed that the value of MSE is minimum for the PO algorithm. Figure 21 represents the fill factors, FF_{po}, FF_{ic}, and FF_{tc}—obtained for PO, IC, and TC algorithms, respectively—at different temperatures and IR. It is observed from this figure that as the IR and temperature are increased, fill factors obtained by all the three algorithms decrease slightly. It is also clear from the figure that, out of the three algorithms, the TC algorithm gives the highest fill factor. Figure 22 presents the internal and overall efficiencies η_{ipo}, η_{opo}, η_{iic}, η_{oic}, η_{itc} and η_{otc} for PO, IC and TC algorithms, respectively. It is observed from this figure that both internal and overall efficiencies for the IC algorithm have the highest values out of all algorithms. For the internal

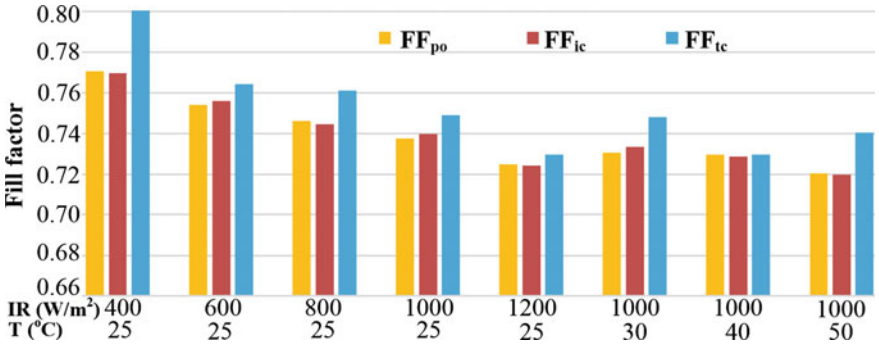

Fig. 21 Fill Factor with PO, IC and TC algorithm when both temperature and irradiance are varied

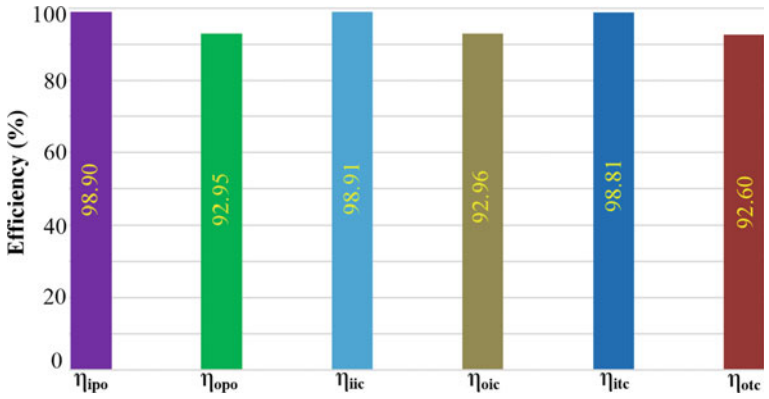

Fig. 22 Internal and overall efficiency with PO, IC and TC algorithm

efficiency calculation, PV output power is considered while for the calculation of overall efficiency, the load output power is considered. That means, for internal efficiency calculation, output power equal to the product of V_{pv} and I_{pv} while for overall efficiency calculation, the output power is equal to the product of V_L and I_L as given in Fig. 3.

7 Conclusion

Three different MPPT techniques (i.e., PO, IC and TC) are tested on PV systems by using MATLAB/Simulink offline simulations. The techniques have been compared in terms of delay time, rise time, peak time, MSE, ripple content in voltage, current, and power, internal efficiency, overall efficiency and fill factor for different IRs and temperatures. It is found that all three MPPT techniques are successfully tracking the MPP and obtained results are comparable. However, for a particular parameter, one technique is found to be superior to another viz., TC method provides a better fill factor, the PO method gives better MSE and the IC method provides better internal and overall efficiencies.

References

1. Qazi A, Hussain F, Rahim NABD, Hardaker G, Alghazzawi D, Shaban K, Haruna K (2019) Towards sustainable energy: a systematic review of renewable energy sources, technologies, and public opinions. IEEE Access 7:63837–63851. https://doi.org/10.1109/ACCESS.2019.2906402
2. Akhtar I, Kirmani S, Jamil M (2019) Analysis and design of a sustainable microgrid primarily powered by renewable energy sources with dynamic performance improvement. IET Renew Power Gener 13:1024–1036. https://doi.org/10.1049/iet-rpg.2018.5117
3. Koraki D, Strunz K (2018) Wind and solar power integration in electricity markets and distribution networks through service-centric virtual power plants. IEEE Trans Power Syst 33:473–485. https://doi.org/10.1109/TPWRS.2017.2710481
4. Hegedus S, Luque A (2011) Achievements and challenges of solar electricity from photovoltaics. In: Handbook of photovoltaic science and engineering. Wiley, pp 1–38. https://doi.org/10.1002/9780470974704.ch1
5. Branker K, Pathak MJM, Pearce JM (2011) A review of solar photovoltaic levelized cost of electricity. https://doi.org/10.1016/j.rser.2011.07.104
6. Singh PP, Singh S (2010) Realistic generation cost of solar photovoltaic electricity. Renew Energy 35:563–569. https://doi.org/10.1016/j.renene.2009.07.020
7. Yang CJ (2010) Reconsidering solar grid parity. Energy Policy 38:3270–3273. https://doi.org/10.1016/j.enpol.2010.03.013
8. Ansari S, Gupta OH, Tripathy M (2021) An islanding detection methodology for SOFC-based static DG using DWT. In: Lecture notes in electrical engineering. Springer Science and Business Media Deutschland GmbH, pp 95–107. https://doi.org/10.1007/978-981-15-7994-3_9
9. Ansari S, Gupta OH (2021) Voltage ripple-based islanding technique on modified IEEE-13 bus test feeder for photovoltaic inverter. In: Lecture notes in electrical engineering. Springer Science and Business Media Deutschland GmbH, pp 139–155. https://doi.org/10.1007/978-981-15-7994-3_13

10. Logeswaran T, SenthilKumar A (2014) A review of maximum power point tracking algorithms for photovoltaic systems under uniform and non-uniform irradiances. Energy Procedia 228–235. https://doi.org/10.1016/j.egypro.2014.07.266
11. Soualmia A, Chenni R (2017) A survey of maximum peak power tracking techniques used in photovoltaic power systems. In: FTC 2016—proceedings of future technologies conference. Institute of Electrical and Electronics Engineers Inc., pp 430–443. https://doi.org/10.1109/FTC.2016.7821645
12. Husain MA, Tariq A, Hameed S, Arif MSB, Jain A (2017) Comparative assessment of maximum power point tracking procedures for photovoltaic systems. https://doi.org/10.1016/j.gee.2016.11.001
13. Balasubrahmanyam CHS, Gupta OH (2020) Detailed study of solar energy conversion system using boost converter—a new MPPT technique. J Inst Eng India Ser B 101:631–639. https://doi.org/10.1007/s40031-020-00478-1
14. Wasynczuk O (1983) Dynamic behavior of a class of photovoltaic power systems. IEEE Power Eng Rev PER-3:36–37. https://doi.org/10.1109/MPER.1983.5519293
15. Hua C, Lin JR (1996) DSP-based controller application in battery storage of photovoltaic system. In: IECON proceedings (industrial electronics conference). IEEE, pp.1705–1710. https://doi.org/10.1109/iecon.1996.570673
16. Hua C, Lin J, Shen C (1998) Implementation of a DSP-controlled photovoltaic system with peak power tracking. IEEE Trans Ind Electron 45:99–107. https://doi.org/10.1109/41.661310
17. Abdelsalam AK, Massoud AM, Ahmed S, Enjeti PN (2011) High-performance adaptive perturb and observe MPPT technique for photovoltaic-based microgrids. IEEE Trans Power Electron 26:1010–1021. https://doi.org/10.1109/TPEL.2011.2106221
18. Bianconi E, Calvente J, Giral R, Mamarelis E, Petrone G, Ramos-Paja CA, Spagnuolo G, Vitelli M (2013) Perturb and observe MPPT algorithm with a current controller based on the sliding mode. Int J Electr Power Energy Syst 44:346–356. https://doi.org/10.1016/j.ijepes.2012.07.046
19. Kumar N, Hussain I, Singh B, Panigrahi BK (2018) Framework of maximum power extraction from solar PV panel using self predictive perturb and observe algorithm. IEEE Trans Sustain Energy 9:895–903. https://doi.org/10.1109/TSTE.2017.2764266
20. Huynh P, Cho BH (1996) Design and analysis of a microprocessor-controlled peak-power-tracking system. IEEE Trans Aerosp Electron Syst 32:182–190. https://doi.org/10.1109/7.481260
21. John R, Mohammed SS, Zachariah R (2018) Variable step size perturb and observe MPPT algorithm for standalone solar photovoltaic system. In: Proceedings of the 2017 IEEE international conference on intelligent techniques in control, optimization and signal processing, INCOS 2017. Institute of Electrical and Electronics Engineers Inc., pp 1–6. https://doi.org/10.1109/ITCOSP.2017.8303163
22. Yu GJ, Jung YS, Choi JY, Choy I, Song JH, Kim GS (2002) A novel two-mode MPPT control algorithm based on comparative study of existing algorithms. In: Conference record of the IEEE photovoltaic specialists conference, pp 1531–1534. https://doi.org/10.1109/pvsc.2002.1190903
23. Hua C, Lin J (2003) An on-line MPPT algorithm for rapidly changing illuminations of solar arrays. Renew Energy 28:1129–1142. https://doi.org/10.1016/S0960-1481(02)00214-8
24. Hussein KH, Muta I, Hoshino T, Osakada M (1995) Maximum photovoltaic power tracking: an algorithm for rapidly changing atmospheric conditions. IEE Proc Gener Transm Distrib 142:59–64. https://doi.org/10.1049/ip-gtd:19951577
25. Liu F, Duan S, Liu F, Liu B, Kang Y (2008) A variable step size INC MPPT method for PV systems. IEEE Trans Ind Electron 55:2622–2628. https://doi.org/10.1109/TIE.2008.920550
26. Mei Q, Shan M, Liu L, Guerrero JM (2011) A novel improved variable step-size incremental-resistance MPPT method for PV systems. IEEE Trans Ind Electron 58:2427–2434. https://doi.org/10.1109/TIE.2010.2064275
27. Zakzouk NE, Elsaharty MA, Abdelsalam AK, Helal AA, Williams BW (2016) Improved performance low-cost incremental conductance PV MPPT technique. IET Renew Power Gener 10:561–574. https://doi.org/10.1049/iet-rpg.2015.0203

28. Alsumiri M (2019) Residual incremental conductance based nonparametric MPPT control for solar photovoltaic energy conversion system. IEEE Access 7:87901–87906. https://doi.org/10.1109/ACCESS.2019.2925687
29. Mutoh N, Matuo T, Okada K, Sakai M (2002) Prediction-data-based maximum-power-point-tracking method for photovoltaic power generation systems. In: PESC record—IEEE annual power electronics specialists conference, pp 1489–1494. https://doi.org/10.1109/psec.2002.1022386
30. Park M, Yu IK (2004) A study on the optimal voltage for MPPT obtained by surface temperature of solar cell. In: IECON proceedings (industrial electronics conference), pp 2040–2045. https://doi.org/10.1109/iecon.2004.1432110
31. Swaraj K, Mohapatra A, Sahoo SS (2017) Combining PV MPPT algorithm based on temperature measurement with a PV cooling system. In: International conference on signal processing, communication, power and embedded system, SCOPES 2016—proceedings. Institute of Electrical and Electronics Engineers Inc., pp 482–489. https://doi.org/10.1109/SCOPES.2016.7955876
32. Coelho RF, Concer FM, Martins DC (2010) A MPPT approach based on temperature measurements applied in PV systems. In: 2010 IEEE international conference on sustainable energy technologies, ICSET 2010. https://doi.org/10.1109/ICSET.2010.5684440